JOURNAL OF OPTOELECTRONICS AND ADVANCED MATERIALS, Vol. 11, No. 1, January 2009, p. 70 - 75

AFM investigations of calcium hydroxyapatite thin films on the surface of thin silica films

B. ČOLOVIĆ, V. JOKANOVIĆ*, B.MARKOVIĆ-TODOROVIĆ, Z. MARKOVIĆ[a]
Institute of Nuclear Sciences "Vinča", Laboratory for Radiation Physics and Chemistry, Mike Petrovića Alasa 12-14, 11001 Belgrade, Serbia
[a]*Institute of Nuclear Sciences "Vinča", Atomic Physics Laboratory, Mike Petrovića Alasa 12-14, 11001 Belgrade, Serbia*

The synthesis of calcium hydroxyapatite in a slightly modified SBF fluid by self-assembly on the surfaces of SiO_2 thin films was investigated in this study. The mechanism of their nucleation on the surface of silica thin films of various depths was particullarly investigated by using AFM. The analysis of the obtained phases after different times of sample ageing in modified SBF was determined using the FTIR-ATR method. The thicknesses of the film were investigated over the mass changes of the samples. The corresponding corrections related to the total pore volume inside of them were included in the final results of their thicknesses.

(Received January 5, 2009; accepted January 21, 2009)

Keywords: Calciumhydrohyapatite, Thin films, SiO_2 substrate, Steel tape, Mechanism of biomimetic CHA self-nucleation, IR spectroscopy, AFM, BET volume correction

1. Introduction

Most dental and orthopaedic implants contain titanium and its alloys or some other metals like stainless steel because they have a relatively good biocompatibility, resistance to corrosion, mechanical properties and workability.[1] However, if implants were applied without ceramic base coatings, the bone implant failure, due to incomplete osteointegration [2]. The success of an implantantion primarly depends on the ability of the material to create a bond with the living host tissue, which is strongly affected by the chemical and physical properties of the surface [3]. Improvement of fixation between hard tissues and implants can be achieved only by coating of the metal surface with a thin film of calcium phosphates [4-6]. In fact, calcium phosphates are bioactive and osteoconductive, and promote direct attachment to the bone. The deposition of coating on metal implant can be made by one of the numerous physical and chemical methods, including plasma spraying, magnetron sputtering, ion-beam coating, electrophoretic deposition, anode oxidation, anodic spark deposition, and pulsed laser ablation [7-17].

Among them, biomimetic method of apatite deposition, based on the use of supersaturated solutions with an ionic composition similar to that of human plasma is highly promising. These methods generally show reduced adhesion to the metallic substrate [18,19]. Nevertheless, they have numerous advantages, including the possibility to coat complex shaped materials and coprecipitate biologically active molecules together with apatitic crystals onto the implant surface. Furthermore, the inorganic phase deposited from supersaturated solutions has chemical, morphological and structural properties like to the natural bone [20].

The interest to use SBF for preparation of biomimetic apatite coatings has greatly increased within the last years [21-25]. Thus, several SBF solutions such as modified (m-SBF) with ionic concentrations closer or equal to that of human blood plasma have been prepared [26].

The synthesis of such coatings which is very like to the natural bone, still remains one of the most interesting topics of the advanced technological research. Hence, much attention has been recently devoted to the development of new biomimetic coatings contained from the non-stoichiometric apatites, which can assure higher rate of biodegradability and bioactivity of hydroxyapatites compared to stoichiometric hydroxyapatite.

This line of research is a consequence of a better comprehension of the functional role of the active groups contained in the natural bone tissue at physiological conditions, such as a crystallinity grade of powders and addition of doping components into them to order to make it comparable to the natural bone tissues.

Nevertheless, of the chosen kind of coatings, ceramic materials such as SiO_2 and TiO_2 deposited on a metal surface as a coating, can facilitate deposition of calcium ions and thus have been described as inducers of apatite nucleation [27-33].

The present paper reports a study carried out with CHA produced biomimetically using slightly modified SBF [34], as the second layer on a silica surface previously deposited on the surface of a steel tape by twin-fluid spray deposition. The silica thin film has a very suitable activity of surfaces for biomimetic nucleation of CHA on its surface,as it was clearly shown in this research.

2. Experimental

2.1 Deposition of CHA thin films

The deposition of CHA thin films was done by a complex procedure. In the first step, the SiO_2 thin films were deposited on the surfaces of the stainless steel tapes, using movable twin-fluid spray equipment, described in details elsewhere. Briefly, the procedure was as follows. The precursor solution was introduced into a glass nozzle, of diameter 0.2 mm. The flow through the nozzle was adjusted using a peristaltic pump. The liquid precursor was atomized by the introduction of air to the nozzle at a controlled flow rate. Flow rate of the liquid precursor was maintained at 44 ml/h and air flow rate for liquid atomization at 300 l/h. The spray was fully controlled by a self made computer driven device which enabled the nozzle to be moved at chosen speed and direction. The distances between the nozzle and substrate (stainless steel (SS) tape, Sandvik OC 404, thickness 35 μm) were 4 cm and 11 cm, creating a spraying spot on the substrate, of diameter 2.0 cm and 5.5 cm, respectively. A rectangular SS tape, external surface area of 30 cm^2 (3 × 10 cm) was used as the substrate. The nozzle movement was directed parallel to the longer rectangular side of the SS tape and after each pass, the nozzle pathway was shifted by 1 mm in the direction of the shorter rectangular side. The nozzle moved at 1 cm/s.

The initial temperature of the substrate was 420 °C while at the center of the spraying spot, temperature dropped to about 100 °C. The nozzle speed (1 cm/s) provided sufficient time, at least 15 s, for the deposited precursor drops to undergo several consecutive processes: solvent evaporation, precursor precipitation, drying, pyrolysis of precursors, and film growth due to crystallization. This operating mode is similar to the conventional pulse spray pyrolysis method with a fixed nozzle.

The duration of the substrate spraying was varied in the range of 26 to 39 min. As a precursor, a silica sol with SiO_2 concentration of 13.5 wt. % was used.

The finally obtained corresponding depth of the SiO_2 thin films was 22.5 μm.

These specimens were then emerged in the SBF, which had been prepared by a slightly modified recipe, (c_{Cl^-} = 0.054 mol/L; c_{Na^+} = 0.0542 mol/L; $c_{Ca^{2+}}$ = 0.0025 mol/L; $c_{PO_4^{3-}}$ = 0.001 mol/L; $c_{Mg^{2+}}$ = 0.0003 mol/L; $c_{NO_3^-}$ = 0.0006 mol/L and c_{K^+} = 0.0014 mol/L), i.e., a small increase in the concentration of PO_4^{3-} and Ca^{2+} and a decrease in the concentration of Na^+ and Cl^- ions in comparison to their concentrations in the original SBF fluid.

Clearly, the PO_4^{3-} and Ca^{2+} concentrations were shifted slightly over their boundary of the solubility in CHA crystal cell, given by solubility product (PS = 2.34 × 10^{-59}) [35,36].This was provided by a very careful regulation of the concentrations of the PO_4^{3-} and Ca^{2+} ions in the modified SBF solution, by adjusting their concentrations to be a slightly above the solubility boundary of CHA in SBF. These samples in so-modified SBF, were then left to age for various time (10 days, 20 days, 33 days and 43 days) at 37 °C. During the aging, the concentration of the Ca^{2+} ions in SBF solution was periodically verified by atomic spectroscopy, to be balanced closed to the solubility product of CHA. After, ageing, the samples were removed from the SBF, carefully rinsed with deionized water and prepared for subsequent AFM, BET and FTIR-ATR investigations.

2.2. Characterization methods

AFM measurements were performed using Quesant microscope operating in tapping mode in air at the room temperature. In tapping mode the cantilever oscillates close to a resonance and the tip only slightly touches the surface. The morphology and typical structure of SiO_2 thin film and selfassembled CHA film deposed on its surface were investigated by using standard silicon tips (purchased from Nano and more) with constant force of 40 N/m. The accuracy of the AFM mean diameter determination was improved by deconvolution. The mean diameter of investigated particles was determined by Quesant SMP program.

The phase investigations were performed using FTIR-ATR spectroscopy (Nicollet 380 FT-IR, Thermo Electron Corporation).

The nitrogen gas absorption BET method (Sorptomatic 1990, Termoquest CE Instruments) was used for the determination of the specific surface areas of the CHA powders. The samples (0.20 – 0.22 g) for absorption measurement were thoroughly degassed at 150 °C for 3 h. Knowing the absorbed volume of N_2 (purity 99.99 %), the specific surface areas of the CHA powders were determined applying the BET method .Method is based on the correlation $p/(V_{ads}\,(p_o - p))$ vs. p/p_o, where p_o is the saturation pressure, p is the equilibrium pressure and V_{ads} is the absorbed volume of nitrogen. The Dubinin Radushkevich method (correlation $\log(V_{ads})$ vs. $\log_2(p_o/p)$ was used for the determination of the specific surface area, too. The average and the maximum radius of pores and the cumulative volume of all pores were determined using the Lecloux and Pirard method based on the Dollimore Heal Pore-sizes standard absorption isotherm [17].

The concentration of the contained Ca and P was determined using adsorption atomic spectroscopy (Perkin Elmer 3030B). For the preparation of the samples for chemical analysis, a slightly modified procedure described by Connel and Lam was applied. In accordance with the requirement to be close to the boundary of the solubility of Ca^{2+} and PO_4^{3-} in the SBF, small amounts of water were added [37].

3. Results and disscusion

3.1. The SiO_2 thin films on the steel tape substrate

By the spray pyrolysis method, the obtained SiO_2 film has a typical appearance shown in Fig.1.

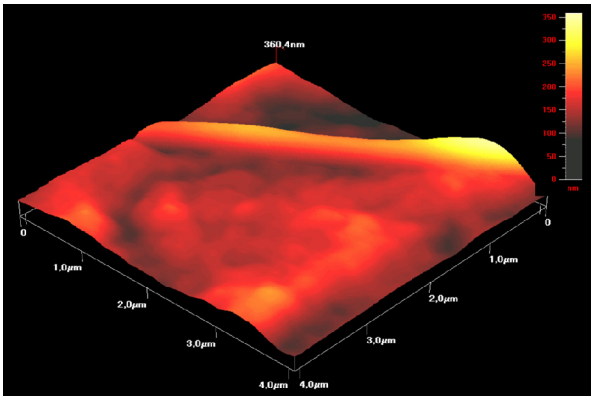

Fig. 1. AFM image of SiO_2 film.

The calculated film thiskness by using the mass change during the spray pyrolysis was 22.5 μm. In this value the correction of the thickness caused by total pore volume was calculated by using the Lecloux and Pirard method based on the Dollimore Heal Pore-sizes standard absorption isotherm [17].

Detailed desciption of this method and results obtained by it can be found elsewhere [17].

3.2. Thickness of the CHA thin films

As it is shown in Table 1. the CHA film masses were dependent of the time ageing of the SiO_2 thin films in slightly modified SBF.

The CHA film thicknesses after corrections of the mass data for the volume of the pores in the films (made by the Lecloux and Pirard method based on the Dollimore Heal Pore-sizes standard absorption isotherm) were calculated from these data and they were in the range of 2.7 – 6.2 μm. The highest value was obtained for a nucleation time of the 43 days (6.2 μm) whilst the smallest, close to zero, was obtained with the nucleation time of 10 days.

Table 1. Thicknesses of the self-nucleated CHA thin films on the surfaces of of SiO_2 thin films

SiO_2 film depth, μm	Time of the HAP nucleation days	Mass of the HAP mg	Specific surfaces, m^2/g	Volume pores, cm^3/g	CHA film thickness μm
22.5	10	0.2	-	-	-
	20	0.6	94	0.116	2.7
	33	1.1	102	0.107	4.9
	43	1.4	112	0.097	6.2

3.3. IR spectroscopy of CHA thin films

The band at about 2340 cm^{-1}, as it can be seen in Fig.2, can be assigned to the OH^- stretching vibration of the OH^- groups placed at both ends of silica chains of SiO_2 sol particles. Detailed description of the structure of these silica chains and their lenght is given in ref. 18. Briefly, using the DTA of silica sol particles, it was found that silica chains are constituted from 16 to 20 silica thetraedra with OH^-groups on the chain ends.

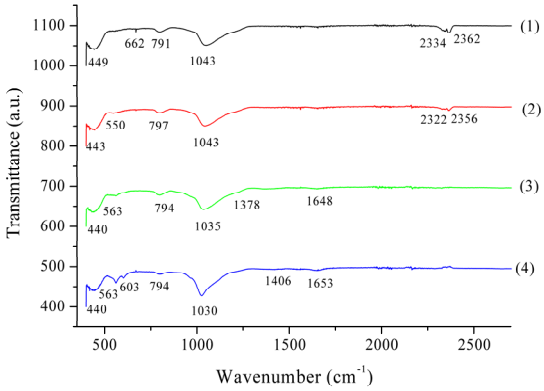

Fig. 2. IR spectra of various hydroxyapatite layers obtained on the surface of SiO_2 thin film depth 22.5 μm by ageing in slightly modified SBF media (1 -ageing time 10 days, 2 - ageing time 20 days; 3- ageing time 33 days; 4- ageing time 43 days).

Therefore, with decreasing hydrogen bond length from 2.928 to 2.893 Å, as described in ref. [38], the wave number of stretching vibration of the OH^- groups can be changed from 2477 cm^{-1} to 2315 cm^{-1}. The observed slightly lower frequency of the OH^- vibration with decreasing hydrogen bond length, by this explanation, may be caused by steric effects. According to this, the fine structure of the OH^- vibration in the spectra probably can be generated by the strong anharmonic coupling mechanism. High frequency proton stretching vibrations has the most prominent role and they are anharmonically coupled with the low frequency hydrogen bond stretching vibration [38].

These vibrations were observed in almost all the samples of CHA but they were more pronounced for the samples which were nucleated in the modified SBF for 10 and 20 days and for the samples on the SiO_2 thin films of smaller thickness. These indirectly may confirm the shortening of the hydrogen bond, which can really be caused by the influence of various impurities contained in SBF (such as for example Na^+ ions previously added to be stabilisator of SiO_2 sol particles in SiO_2 solution) to the OH^- groups of the silica chains. Obviously, that effect is more pronounced for smaller thicknesses of the self-nucleated CHA layers [39-41].

The IR spectra show also bands at 1643 to 1649 cm^{-1} which can be assigned to the bending mode of the OH^- groups contained in both the SiO_2 and CHA thin films.

The bands at 1018 to 1043 cm^{-1} correspond to the transversal asymmetric vibrations of Si-O-Si. The shifting of this value towards a lower wave number value can be an indication of the movement of O atom along the line parallel to the Si-Si axes. In turn this causes a distortion in the surrounding Si-O bonds, bringing about a so-called asymmetric transversal oscillation caused by the cationic shifting. [39-41]

The bands at 791 to 802 cm^{-1} corresponds to the rocking deformation in the Si-O-Si chains caused by coupling the transversal symmetric vibration of the O atom alongside the bisection of the Si-O-Si angle, with the simultaneous movement of Si cations. [40]

Finally, the bands at 432 to 451 cm^{-1} correspond to the transversal optic rocking mode of Si-O-Si, created by stretching vibrations of the O atom regarding the position of the Si atoms in the Si-O-Si chain. [40]

The bands from 1018 to 1043 cm^{-1}, correspond partially to the asymmetric stretching mode of the PO_4^{3-} vibration. Also, the bands at 432 – 451 cm^{-1} partially belong to the ν_2 symmetric stretching mode of the PO_4^{3-} vibration. All of these bands belong to the both the SiO_2 and CHA layers. [39, 41]

Behind of them, very strong pronounced bands at 550 to 563 cm^{-1}, which correspond to the PO_4^{3-} ν2 symmetric stretching vibration, were present. Also, bands corresponding to the liberation mode of the OH^- vibration at 600 to 662 cm^{-1} were observed. The shifting of these vibrations from 630 cm^{-1} to the various above-given values showed that anionic species may have influence to the liberation mode of OH^- vibration in CHA.. The higher values of these wave numbers can be assigned to the higher quantity of the OH^- ions substituted by other ionic species [39,41,42].

2.4. Mechanism of CHA film formation

Because the pH zero point value of silica thin film substrate obtained by using titration method was about 5.7 and modified SBF pH 7.4 it follows that the silica film is negativelly charged. Only in some spots occupied with Na^+ ions, the pH value of zero point of silica thin films may be higher than pH of modified SBF. In these spots, silica thin films are positivelly charged. According to this, the charged film surface and surrounding solution form a thin double layer to which positivelly charged Ca^{2+} was preferentially attracted and inital reaction started between the charged film surface and attracted ions [43]. The next layer will be normally occupied by the oposite negativelly charged PO_4^{3-}.leading to the formation of calcium phosphate. With the formation of calcium apatite on the surface, the supersaturation of slightly modified SBF may promote preferential nucleation of CHA on the already formed apatite then in SBF solution, because the heterogenous reaction needs less energy then homogenous reaction inside of SBF. Thus further formation of the CHA film continues preferentially on the initial CHA layer by spontanous growth consuming Ca^{2+} and PO_4^{3-}ionas from the surrounding SBF. A theroretical analysis [44] indicated that formation of CHA exhibits a higher thermodinamic preference than other phosphate phases like octacalcium-phosphate and dicalcium phosphate.

The next important factor which caused a secondary CHA film nucleation is probably a capillary tension between the islands of the facets, generated by the very small distance between them. This factor influenced a small, mechanical fluid instability which might cause the flow of the fluid between islands of previously nucleated CHA.

The mechanism of slow ion precipitation, layer by layer, cation ions and anion counter ions, was dominant in the phase of the growth of islands and their shaping, while the mechanism of secondary nucleation induced by capillary forces was responsible in the latter phases of film formation through the filling of the channels between the islands (Fig.3). The very small diameters of the channels, which were of the order of several nanometers, induced a corresponding capillary forces sufficient for the flow of the SBF and a sliding of parts of the edges of the facets into the valley of the channels. In this way, bridges between the islands were built.

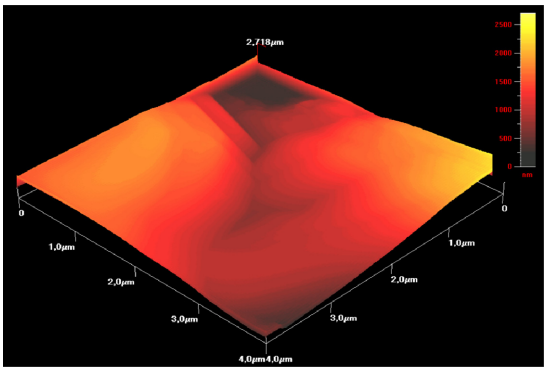

Fig 3. AFM image of CHA film with pronounced facets.

The hydrodynamic force which influenced the movement of the SBF solution in the channels (pronounced valleys) between the islands is probably responsible for a corresponding erosion and replacement of the weakly bonded edges of the facets at the bottom of these channels-valleys between the previously nucleated islands of CHA, as it is shown in Fig 4.

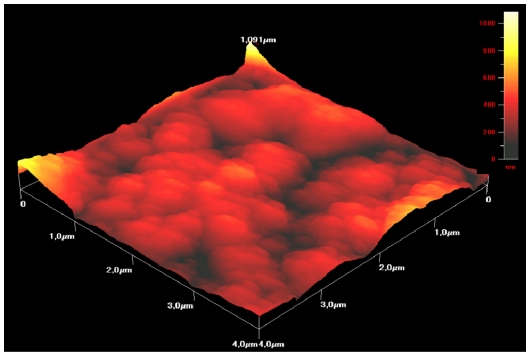

Fig 4. AFM image of CHA secondary film.

Of course, these forces preferently depend on the distance between the islands (diameter of channels). The smaller diameter of channels cause the stronger capillary forces and consequentlly higher capillary pressures inside of the channels, causing the additional erosion of the CHA facet edges and formation of the corresponding CHA bridges among the islands, by the mechanism of secondary nucleation (Fig. 4).

4. Conclusions

In this study, the self-nucleation of CHA from a slightly modified chemical composition SBF on the surfaces of SiO_2 thin films, previously deposited on the surface of stainless steel bands was investigated.

The mechanism of CHA film nucleation is independent of the conditions of their formation. It is influenced preferentially by the concentrations of Ca^{2+} and PO_4^{3-} ions and their solubility products in CHA.

The AFM measurements show a typical structure of the selfassembled CHA film and as it has been shown in the mechanism interpretation enable deeper understanding of different stages of self-assembling.

The IR spectra clearly showed the presence of CHA with a slightly modified structure, shown by the characteristics bands being more or less shifted to higher values of the corresponding wave numbers, compared to the values for their "ideal" positions.

References

[1] M. Niinomi, Metall Mater Trans A **33**, 477 (2002).
[2] T. J. Webster, Nanophase ceramics: the future of orthopedic and dental implant material. In: Ying JY, editor. Nanostructured materials. New York: Academic Press; (2001), 125-166.
[3] A. Bigi, M. Fini, B. Bracci, E. Boanini, P. Torricelli, G. Giavaresi, N. Aldini, A. Facchini, F. Sbaiz, R, Giardino Biomaterials **29**, 1730 (2008).
[4] Eng San Thian, Jie Huang, Serena M Best, Zoe H Barber, Roger A Brooks, Neil Rushton, William Bonfield, Biomaterials, **27**, 2692 (2006).
[5] T Kokubo, H Takadama, Biomaterials **27**, 2907 (2006).
[6] R. Z. LeGeros, Clin Orthop Relat Res, **395**, 81 (2002).
[7] L. Sun, C. C. Berndt, K. A. Gross, A. Kucuk, J. Biomed Mater Res Appl Biomat , **58**, 570 (2001).
[8] G. Socol, P. Torricelli, B. Bracci, M. Iliescu, F. Miroiu, A. Bigi, et al. Biomaterials, **25**, 2539 (2004).
[9] J. G. C. Wolke, J. P. C. M. van der Waerden, H. G. Schaeken, J. A. Jansen. Biomaterials **24**, 2623 (2003).
[10] Z. S. Luo, F. Z. Cui, W. Z. Li, J. Biomed Mater Res, **46**, 80 (1999).
[11] M. Wei, A. J. Ruys, B. K. Milthorpe, C. C. Sorrell, Solution J.Biomed Mater Res, **45**, 11 (1999).
[12] E. S. Thian, J. Huang, S. M. Best, Z. H. Barber, W. Bonfield, Mat.Sci.Eng.:C, **27**, 251 (2007).
[13] R. Chiesa, E. Sandrini, M. Santin, G. Rondelli, A. Cigada, J. Appl. Biomater Biomech, **1**, 91 (2003) .
[14] A. Bigi, B. Bracci, F. Cuisinier, R. Elkaim, R. Giardino, I. Mayer, et al. Biomaterials **26,** 2381 (2005).
[15] P. Li, C. Ohtsuki, T. Kokubo, K. Nakanishi, N. Soga, T. Nakamura, et al. J Biomed Mater Res **28,** 7 (1994).
[16] V. Jokanović, D. Uskoković, Mat.Trans. JIM **46**, 228 (2005).
[17] V. Jokanović, B. Jokanović, D. Izvonar, B. Dačić, J. Mater. Sci. Mat.in Medicine, 8 (2008) 1871-1879.
[18] A. C. Tas, Biomaterials, **21**, 1429 (2000).
[19] F. Barrere, C. M. van der Valk, R. A. J. Dalmeijer, C. A. van Blitterswijk, K. de Groot, P. Layrolle, J Biomed Mater Res **64**, 378 (2003).
[20] A. Bigi, E. Boanini, B. Bracci, A. Facchini, S Panzavolta, F. Segatti et al., Biomaterials, **26**, 4085 (2005).
[21] F. A. Muller, L. Jonasova, P. Cromme, C Zollfrank, P. Greil, Key Eng Mater **254–256**, 1111 (2004).
[22] F. Barrere C. A. van Blitterswijk, K. de Groot, P. Layrolle, Biomaterials **23**, 1921 (2002).
[23] F. Barrere, C. A. van Blitterswijk, K. de Groot, P. Layrolle, Biomaterials, **23**, 2211 (2002).
[24] P. Li, C. Ohtsuki, T. Kokubo, J. Am. Ceram Soc **75**, 2094 (1992).
[25] L. Muller, F. A. Muller, Acta Biomaterialia **2,** 181 (2006).
[26] A. Oyane, H. K. Kim, T. Furuya, T. Kokubo, T. Miyazaki, T. Nakamura, J. Biomed. Mater. Res. **65A**, 188 (2003).
[27] E.S. Thian, J. Huang, S. M. Best, Z. H. Barber, W. Bonfield, Mat.Sci.Eng.:**C27,** 251 (2007).
[28] Y. Li, W. Weng, J. Mat. Sci.: Mat. in Medicine, **19,** 19 (2008).
[29] L. L. Hench, R. J. Splinter, W. C. Allen, J Biomed Mater.Res **2**, 117 (1972).
[30] A. Oyane, K. Onuma, A. Ito, H. M. Kim, T. Kokubo, T. Nakamura, J Biomed Mater Res, **64A,** 339 (2003).
[31] S. Cho, Nakanishi K, Kokubo T, Soga N, Ohtsuki C, Nakamura T,et al. J Am Ceram Soc **78**, 1769 (1995).
[32] P. Li, C. Ohtsuki, T. Kokubo, K. Nakanishi, N. Soga, T. Nakamura, et al. J Biomed Mater Res **28,** 7 (1994).
[33] M. Neo, T. Nakamura, C. Ohtsuki, T. Kokubo, T. Yamamuro, J Biomed Mater Res;**27,** 999 (1993).
[34] M. Uchida, H. M. Kim, T. Kokubo, T. Nakamura, J. Am Ceram Soc **84**, 2041 **(**2001).
[35] L. Muller, F. A. Muller, Acta Biomaterialia, **2**, 181 (2006).
[36] A. Oyane, H. K. Kim, T. Furuya, T. Kokubo, T. Miyazaki, T. Nakamura, J. Biomed Mater Res, **65A**, 188 (2003).
[37] J. C. W. Lam, S. Tanabe, S. K. F.Chan, M. H. W. Lam, M. Martin, P. K. S. Lam, Environmental Pollution **144**, 790 (2006).
[38] M. Szafran, J. Koput, Z. Dega-Szafran, A. Katrusiak, J. Mol. Struct. **797,** 66 (2006).

[39] V. Jokanović, D. Uskoković, Mat.Trans. JIM **46**, 228 (2005).
[40] V. Jokanović, B. Jokanović, D. Izvonar, B. Dačić, J. Mater. Sci. Mat.in Medicine, **8**, 1871 (2008).
[41] V. Jokanović , D.Izvonar, M. D.Dramićanin, B. Jokanović, V. Živojinović, D. Marković, B. Dačić, J. Mater. Sci.:Mat. in Medicine **17,** 539 (2006).
[42] J. Xie, B. L. Luan, J. Wang, X. Y. Liu, C. Rorabeck, R. Bourne, Surf.Coat.Techn.**202**, 2960 (2008).
[43] X. Lu, Y. Leng, Biomaterials **26**, 1097 (2005).
[44] I. Grenthe, H. Wanner, (Minor revisions by Östhols E.), Guidelines for the extrapolation to zero ionic strength**, (**2000), Le Seine-St. Germain, 4-29.

*Corresponding author: vukomanj@beotel.net;
vukoman@vin.bg.ac.yu